Type 1 ribosome-inactivating proteins are the most abundant proteins in iris (*Iris hollandica* var. Professor Blaauw) bulbs: characterization and molecular cloning

Els J. M. VAN DAMME*‖, Annick BARRE†, Luigi BARBIERI‡, Paola VALBONESI‡, Pierre ROUGE†, Fred VAN LEUVEN§, Fiorenzo STIRPE‡ and Willy J. PEUMANS*

*Laboratory for Phytopathology and Plant Protection, Catholic University of Leuven, Willem de Croylaan 42, 3001 Leuven, Belgium, †Institut de Pharmacologie et Biologie Structurale, Université Paul Sabatier, 35 Chemin des Maraîchers, UPR CNRS 9062, 31062 Toulouse Cedex, France, ‡Dipartimento di Patologia sperimentale, Università di Bologna, Via S. Giacomo 14, I-40126 Bologna, Italy, and §Center for Human Genetics, Catholic University of Leuven, Herestraat 49, 3001 Leuven, Belgium

The most abundant protein of *Iris* bulbs has been identified as a type 1 ribosome-inactivating protein (RIP). Analysis of the purified proteins and molecular cloning of the corresponding cDNAs demonstrated that this type 1 RIP is a mixture of three isoforms that exhibit a high degree of sequence identity and have similar, though not identical, ribosome-inactivating and polynucleotide:adenosine glycosidase activities. The accumulation of large quantities of type 1 RIP in a vegetative storage organ suggests that this presumed defence-related protein also plays a role in the nitrogen-storage metabolism of the bulb.

INTRODUCTION

Numerous plant species contain proteins, which by virtue of their highly specific RNA N-glycosidase activity are capable of catalytically inactivating ribosomes [1]. According to the generally accepted ideas, the so-called ribosome-inactivating proteins (RIPs) remove a single adenine residue from a conserved loop present in the large ribosomal RNA [2]. Recent work, however, has demonstrated that some, and possibly all, RIPs remove adenine residues from different polynucleotides such as RNA, DNA and poly(A), and hence behave as polynucleotide:adenine glycosidases [3–6]. RIPs are usually divided in two subgroups with a different molecular structure. Type 1 RIPs consist of a single polypeptide chain of approx. 30 kDa. In contrast, type 2 RIPs contain catalytically active A-chains and carbohydrate-binding B-chains. Both chains are derived from a single precursor by the excision of a linker sequence between the A and B domain and are held together by a disulphide bridge between cysteine residues at the C-terminus of the A domain and the N-terminus of the B domain.

In the past numerous type 1 RIPs have been isolated and characterized in some detail. Type 1 RIPs are a homogeneous family of proteins with regard to their biochemical properties and primary structure but differ from each other with respect to their enzymic properties and biological activities. Since there is still a broad interest in type 1 RIPs because of their potential use as plant resistance factors against viruses and fungi, and their possible therapeutic applications as biomissiles, the search for novel type 1 RIPs with interesting properties continues. At present, the majority of type 1 RIPs have been isolated from dicotyledonous plants of the families Cucurbitaceae, Chenopodiaceae, Caryophyllaceae, Euphorbiaceae, Nyctaginaceae, Phytolaccaceae and Lauraceae. Until now, the occurrence of similar proteins in monocotyledonous species has only been documented for a few Gramineae species and for *Asparagus officinalis* (Asparagaceae, Liliales). Therefore the isolation and characterization of novel type 1 RIPs from other monocots will be of great interest to further corroborate the biological activities and molecular evolution of the whole group of type 1 RIPs.

In this paper we report the isolation, characterization and molecular cloning of three closely related type 1 RIPs from the bulbs of *Iris hollandica* (Iridaceae, Liliales). The identification of the most abundant bulb protein as a type 1 RIP not only demonstrates for the first time the occurrence of large quantities of such proteins in a typical vegetative storage organ, but also re-addresses the question of their possible physiological role.

EXPERIMENTAL

Materials

Iris (*Iris hollandica* var. Professor Blaauw) bulbs were purchased from a local store. Oligo(deoxythymidine)–cellulose was purchased from Sigma Chemical Co. Radioisotopes were obtained from ICN. A cDNA synthesis kit, restriction enzymes and DNA modifying enzymes were obtained from Pharmacia LKB Biotechnology Inc. *Escherichia coli* XL1 Blue competent cells were purchased from Stratagene.

Isolation and separation of three type 1 RIPs from *Iris* bulbs

Dry *Iris* bulbs (200 g) were stripped of their sclerotized outer layer and homogenized in 1 litre of 20 mM acetic acid using a Waring blender. The homogenate was squeezed through cheesecloth, centrifuged at 3000 ***g*** for 10 min and the supernatant adjusted to pH 3.0 with 1 M HCl. After standing overnight in the cold room (2 °C), the extract was recentrifuged (3000 ***g*** for 10 min). The supernatant was filtered through Whatman 3MM filter paper, diluted with an equal volume of distilled water and loaded on to a column (5 cm × 5 cm; 100 ml bed volume) of S Fast Flow (Pharmacia, Uppsala, Sweden) equilibrated with 20 mM acetic acid. After loading the proteins, the column was washed with 20 mM sodium formate (pH 3.8) until the A_{280} fell below 0.01. The proteins were eluted with 0.2 M NaCl in 0.5 M

Abbreviations used: HCA, hydrophobic cluster analysis; RIP, ribosome-inactivating protein.

‖ To whom correspondence should be addressed.

The new nucleotide sequences reported in this paper have been submitted to Genbank/EMBL/DDBJ under the accession numbers U78039, U78040 and U78041.

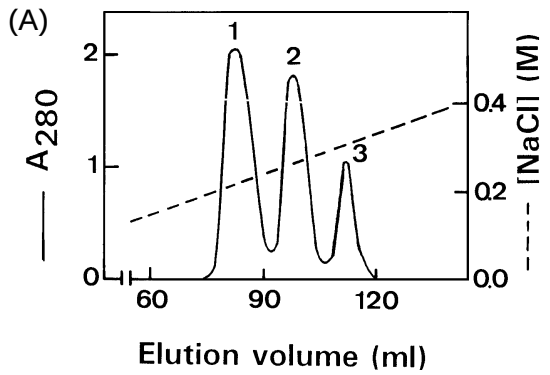

(B)

IETVQ-FRVTG-TTRQT-YSAFL: 30 kDa peak 1

IETVQ-FRVTG-TTRQS-YSAFL: 30 kDa peak 2

IETVE-FRVTG-TTRRS-YSDFL: 30 kDa peak 3

Figure 1 Ion-exchange chromatography and N-terminal sequences of *Iris* type 1 RIPs

(**A**) Ion-exchange chromatography of a total preparation of *Iris* type 1 RIPs on a Neobar CS15/4 column. Details are described in the Experimental section. (**B**) N-terminal amino acid sequences of the proteins eluted in peaks 1, 2 and 3 of (**A**).

Tris/HCl, pH 8.7, dialysed against water, freeze-dried and dissolved in 20 ml of PBS (1.5 mM KH_2PO_4/10 mM Na_2HPO_4/3 mM KCl/140 mM NaCl, pH 7.4). Insoluble material was precipitated by centrifugation at 12000 ***g*** for 10 min and the supernatant chromatographed on a column (40 cm × 5 cm; 800 ml bed volume) of Sephacryl 100 equilibrated with PBS. Fractions of the main peak were pooled, dialysed against water, freeze-dried and redissolved in 20 ml of 20 mM sodium formate (pH 3.8). Aliquots of 5 ml (containing approx. 20 mg protein) were loaded on to a semi-preparative Neobar CS15/4 column (Dynochrom, Lillestrom, Norway) using a Pharmacia FPLC system. After washing the column with 12 ml of buffer, proteins were eluted with a linear gradient (168 ml) of increasing NaCl concentration (0–0.5 M, in the same buffer) at a flow rate of 6 ml/min. Top fractions of the three peaks (Figure 1) were collected and used for further analysis.

Gel filtration

Analytical gel filtration of the purified proteins was performed on a Pharmacia Superose 12 column (type HR 10/30) using PBS containing 0.2 M galactose as the running buffer. Molecular-mass reference markers were catalase (240 kDa), *Ricinus communis* agglutinin (120 kDa), ricin (60 kDa), chymotrypsinogen (25 kDa) and cytochrome *c* (12.5 kDa).

Analytical methods

Total neutral sugar was determined by the phenol/H_2SO_4 method [7], with D-glucose as standard.

Extracts and purified proteins were analysed by SDS/PAGE using 12.5–25% (w/v) acrylamide gradient gels as described by Laemmli [8].

Amino acid sequence analysis

Samples of purified RIP were separated by SDS/PAGE as described above and electroblotted on a PVDF membrane. Polypeptides were excised from the blots and sequenced on an Applied Biosystems model 477A protein sequencer interfaced with an Applied Biosystems model 120A on-line analyser.

Cell-free protein synthesis in a reticulocyte lysate

The effect of RIP on protein synthesis in a cell-free system (a rabbit reticulocyte lysate) was studied essentially as described previously [9]. Reaction mixtures contained, in a final volume of 62.5 μl: 10 mM Tris/HCl, pH 7.4, 100 mM ammonium acetate, 2 mM magnesium acetate, 1 mM ATP, 0.2 mM GTP, 15 mM phosphocreatine, 3 μg of creatine kinase, 0.05 mM amino acids (minus leucine), 89 nCi of L-[^{14}C]leucine, and 25 μl of rabbit reticulocyte lysate. Incubation was at 28 °C for 5 min. Protein synthesis by cells was determined as in Ferreras et al. [10]. The IC_{50} was calculated by linear-regression analysis. Control values were from 4000 to 5000 d.p.m. in different experiments.

Determination of polynucleotide:adenosine glycosidase activity

The polynucleotide:adenosine glycosidase activity was determined by measuring adenine released from various substrates by HPLC [11] essentially following the procedure of McCann et al. [12] as described by Barbieri et al. [4]. Reactions were run for 40 min at 30 °C in a final volume of 50 μl containing 50 mM sodium acetate, pH 4.0, 100 mM KCl, 10 pmol of *Iris* protein and 20 μg of polynucleotidic substrate. Ribosomes (40 pmol) were incubated with 10 pmol of *Iris* protein in a final volume of 50 μl, for 40 min at 30 °C in 7 mM magnesium acetate, 100 mM ammonium chloride, 20 mM Tris/HCl buffer, pH 7.8, 1 mM dithiothreitol. Controls were run without RIP, and a standard curve of adenine was run with each experiment.

RNA isolation

Young shoots were dissected from the inner part of the dry bulbs and finely ground in liquid N_2. Total cellular RNA was prepared essentially as described by Van Damme and Peumans [13]. Poly(A)-rich RNA was isolated by affinity chromatography on oligo(deoxythymidine)–cellulose.

Construction and screening of cDNA library

A cDNA library was constructed with poly(A)-rich mRNA from young *Iris* shoots using the cDNA synthesis kit from Pharmacia. cDNA fragments were inserted into the *Eco*RI site of PUC18. The library was propagated in *E. coli* XL1 Blue (Stratagene).

The cDNA library was initially screened with a ^{32}P-labelled synthetic oligonucleotide derived from the N-terminal sequence of the most prominent type 1 RIP from *Iris*. In a later stage, cDNA clones encoding the type 1 RIP from *Iris* were used as probes to screen for more cDNA clones. Hybridization was carried out overnight as described previously [14]. After washing, filters were blotted dry, wrapped in Saran Wrap and exposed to Fuji film overnight at −70 °C. Positive colonies were selected and rescreened at low density using the same conditions. Plasmids were isolated from purified single colonies on a miniprep scale using the alkaline lysis method as described by Mierendorf and Pfeffer [15] and sequenced by the dideoxy method [16]. DNA sequences were analysed by using programs from PC Gene (Biomed, Geneva, Switzerland) and Genepro (Riverside Scientific, Seattle, WA, U.S.A.).

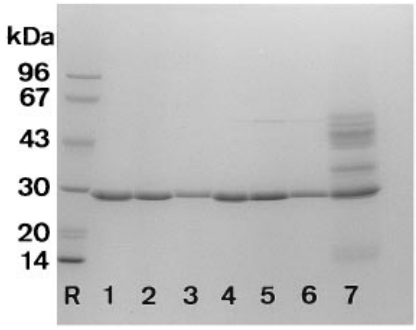

Figure 2 SDS/PAGE of a crude extract and purified type 1 RIPs from *Iris* bulbs

Reduced (with 2-mercaptoethanol) (lanes 1–3) and non-reduced (lanes 4–7) samples were run as follows: lanes 1 and 4, IrisRIP.A1; lanes 2 and 5, IrisRIP.A2; lanes 3 and 6, IrisRIP.A3; lane 7, crude extract from *Iris* bulbs. Molecular-mass reference proteins are shown in lane R; they are lysozyme (14 kDa), soybean trypsin inhibitor (20 kDa), carbonic anhydrase (30 kDa), ovalbumin (43 kDa), BSA (67 kDa) and phosphorylase *b* (96 kDa).

Northern blot

RNA electrophoresis was performed according to Maniatis et al. [17]. Approx. 3 μg of poly(A)-rich RNA was denatured in glyoxal and DMSO and separated in a 1.2 % (w/v) agarose gel. Following electrophoresis the RNA was transferred to Immobilon N membranes (Millipore) and the blot hybridized using a random-primer-labelled cDNA insert as described previously [14]. An RNA ladder (0.16–1.77 kb) was used as a marker.

Molecular modelling

Hydrophobic cluster analysis (HCA) [18,19] was performed to delineate the structurally conserved regions along the amino acid sequences of the type 1 RIP from *Iris* and the A-chain of ricin, which was used as a model. HCA plots were generated on a Macintosh LC using the program HCA-Plot2 (Doriane, Paris, France). Molecular modelling of IrisRIP.A3 was performed on a Silicon Graphics Iris 4D25G workstation, using the programs InsightII, Homology and Discover (Biosym Technologies, San Diego, CA, U.S.A.). The atomic co-ordinates of ricin (code 2aai) were taken from the Brookhaven Protein Data Bank [20] and used to build the three-dimensional model of IrisRIP.A3. Energy minimization and relaxation of the loop regions were carried out by several cycles of steepest descent and conjugate gradient using the cvff forcefield of Discover. The program TurboFrodo (Biographics, Marseille, France) was run on a Silicon Graphics Indigo R3000 workstation to perform the superimposition of the models.

The amino acid sequence alignments were carried on a MicroVAX 3100 (Digital, Evry, France) using the ialign program of PIR/NBRF. The program SeqVu (Gardner, J., 1995, The Garvan Institute of Medical Research, Sydney, Australia) run on the Macintosh LC 630 was used to compare the amino acid sequences of the A-chains of various RIPs. The MacClade program [21] was run on the Macintosh LC630 to build a parsimony phylogenetic tree relating the different RIPs.

RESULTS

Isolation and characterization of three isoforms of a type 1 RIP from *Iris* bulbs

Using a combination of extraction at low pH, ion-exchange chromatography and gel filtration, a pure preparation of a type 1 RIP was isolated from resting *Iris* bulbs. Using ion-exchange chromatography on a Neobar CS15/4 column, the total preparation was further resolved into three isoforms designated IrisRIP.A1, IrisRIP.A2 and IrisRIP.A3 following the elution position from the column (Figure 1). All three isoforms migrated as single polypeptide bands of 29 kDa upon SDS/PAGE (Figure 2) and were eluted with an apparent molecular mass of approx. 30 kDa upon gel filtration on a Superose 12 column (results not shown), indicating that they are single-chain proteins. No covalently bound carbohydrate could be detected in any of the three RIP isoforms by the phenol/sulphuric acid method.

N-terminal amino acid sequencing of the three isoforms revealed highly similar amino acid sequences (Figure 1). In addition, the sequences clearly exhibit sequence similarity to other type 1 and type 2 RIPs.

SDS/PAGE further indicated that the most abundant bulb protein co-migrated with the type 1 RIP (Figure 2). Sequencing of the 29 kDa polypeptide from the crude extract yielded a sequence identical with those of the purified RIPs (results not shown), which confirmed that RIPs are the most abundant proteins in the *Iris* bulb. The abundance of RIPs in a bulb extract can explain the high yield of purified proteins, which was approx. 250 mg of a mixture of the three isoforms from 100 g of bulbs.

Ribosome-inactivating activity of the *Iris* RIPs

All three isoforms inhibited protein synthesis by a reticulocyte lysate. Their activity was similar, the IC_{50} ranging from 0.10 to 0.16 nM (Table 1).

The three isoforms also released adenine, not only from whole

Table 1 Enzymic activity of type 1 RIPs from *Iris*

Inhibition of translation was studied in a lysate of rabbit reticulocytes, and polynucleotide:adenosine glycosidase activity was determined by the release of adenine from various substrates.

		Adenine released (pmol/pmol of enzyme)	(pmol/pmol of enzyme)	(pmol/pmol of enzyme)	(pmol/pmol of substrate)	
Isoform	Substrate ...	hsDNA	rRNA	Poly(A)	Rat liver ribosomes	Inhibition of translation (lysate of rabbit reticulocyte) IC_{50} (nM)
IrisRIP.A1		76	2	2	0.84	0.16
IrisRIP.A2		124	5	5	0.97	0.12
IrisRIP.A3		139	9	3	0.86	0.10

```
RIPIriHol.A1 :    kvnMKTWLILAVTCILWATIAGPVAS▼1IETVQFRVTGTTRQTYSAFL  20
RIPIriHol.A2 :    gvnMKMWLILAVTCVLWATIAGPVAS IETVQFRVTGTTRQSYSAFL
RIPIriHol.A3 :    gvnMKMWLILAVTWILWATIVGPVAS IETVEFRVTGTTRRSYSDFL
                     ** ******* .*****.***** ****.********..**.**

RIPIriHol.A1 :  QTLRTRLSSGSSVHDIPLLPAQSGSQQDLLLVQLFWDDNTPITLVLNR  68
RIPIriHol.A2 :  QNLRTRLSSGTSVHDIPLLPAQSGSQQDLLLVQLFWDDNTPITLVLNR
RIPIriHol.A3 :  QNLRNRLSSGTSVHDIPLLPAQSGSQQDLLFVRLFWDGNRPITLVLNR
                *.**.*****.********************.*.****.* ********

RIPIriHol.A1 :  VNAYLVAYQAKNRYYLLSDTPANPQLYGSNPHRLSFTGSYIALQNVAK 116
RIPIriHol.A2 :  VNAYLVAYQAKNRYYLLSDTPANPQFYGSNPHRLSFTGSYGALQNVAK
RIPIriHol.A3 :  VNAYVVAYQAQNRFYLLADTPANPQVYGNNPHRLTFIGSYGALQNVAK
                ****.*****.**.***.******* **.*****.*.*** *******

RIPIriHol.A1 :  TSRENIDLGINPLATAITTLHNWAPPTVETSVARSLIVLIQLVSETAR 164
RIPIriHol.A2 :  ANRENIDLGINQLATAITTLHNWAPPTVETSVARSLIVLIQLVSETAR
RIPIriHol.A3 :  QNRENIDLGINPLATAISTLHNWSPPTVETSVARSLIVLIQLVSETAR
                 .*********.*****.*****.************************

RIPIriHol.A1 :  FRAIEQRVTSSIIDAVTPIRYDSFRPGVGIIDLQTNWQTLSTEVQRAE 212
RIPIriHol.A2 :  FRAIEQRVTSSIIEAVTPIRYDSFRPGVGIIDLQTNWQTLSTEVQRAE
RIPIriHol.A3 :  FRAIEQRVTNNIIDQVTPIRYDNFRPSVGIIDLQTNWQTLSTEVQRAE
                *********..**..*******.***.************************

RIPIriHol.A1 :  QGIFLQPVKLQVSPQQTVVIGDVEKARTFCGLALLLRWRPSQASLSSH 260
RIPIriHol.A2 :  QGRFLQPVKLQVSPQQTVVIGDVEKARTFCGLALLLRWRPSQASLSSH
RIPIriHol.A3 :  GGRFLQPVKLQVSVQQTVVISDVEKARTFCGLALLLRWRPSQASLSSH
                 * ********** ******.*************************

RIPIriHol.A1 :  DFAWRDLNIRSMLHMGA 277
RIPIriHol.A2 :  DFAWRDLNIRPMLHMGA
RIPIriHol.A3 :  DFAWRD..IRSILDIGA
                ******  **..*..**
```

Figure 3 Comparison of the deduced amino acid sequences of the cDNA clones encoding the type 1 RIPs from *Iris*

The arrowhead indicates the processing site for the cleavage of the signal peptide. Dots denote gaps introduced to get maximal alignment of the sequences. Determined N-terminal amino acid sequences are underlined. Since the first methionine is most probably used as the translation initiation site, the amino acids preceding this methionine are shown in lower case letters. Amino acids that are conserved between the different *Iris* sequences are indicated by asterisks and chemically similar amino acids are indicated by dots on the bottom line.

rat liver ribosomes, but also from purified rRNA, poly(A) and DNA (Table 1). Only one adenine was removed per ribosome. It should be noted that the three isoforms exhibit some differences in their polynucleotide:adenosine glycosidase activity depending on the substrate.

Molecular cloning of cDNAs encoding the three RIPs

Screening of a cDNA library constructed with RNA from young *Iris* shoots resulted in the isolation of three groups of cDNAs. Each of these groups could be assigned to one of the three RIP isoforms on the basis of a perfect match with the N-terminal amino acid sequences of the purified proteins. Sequence analysis indicated that RIPIriHol.A1 (cDNA encoding the type 1 RIP from *Iris*) contains an open reading frame of 908 bp encoding a 303-amino-acid precursor with one putative initiation codon at position 4 of the deduced amino acid sequence (Figure 3). Translation starting with this methionine residue results in a protein of 300 amino acids with a calculated molecular mass of 33.4 kDa. According to the rules of von Heijne [22], a signal peptide is cleaved between residues 23 and 24. The resulting polypeptide, which matches perfectly the N-terminal sequence of IrisRIP.A1, has a molecular mass of 30.9 kDa and an isoelectric point of 9.70. RIPIriHol.A2 and RIPIriHol.A3 show the same overall structure as RIPIriHol.A1 and exhibit 84–95 % sequence identity at the deduced amino acid level. The calculated molecular masses of the isoforms 2 and 3 (after removal of the signal peptide) are 31.0 and 30.9 kDa respectively, and their isoelectric points 9.88 and 9.97 respectively. The isoelectric-point values of the three proteins are in agreement with the sequence of their elution from the cation-exchange column.

Northern blot analysis

Northern blot analysis was performed to determine the total length of the RIP mRNAs. Hybridization of the blot using the synthetic oligonucleotide as a probe yielded one band of approx.

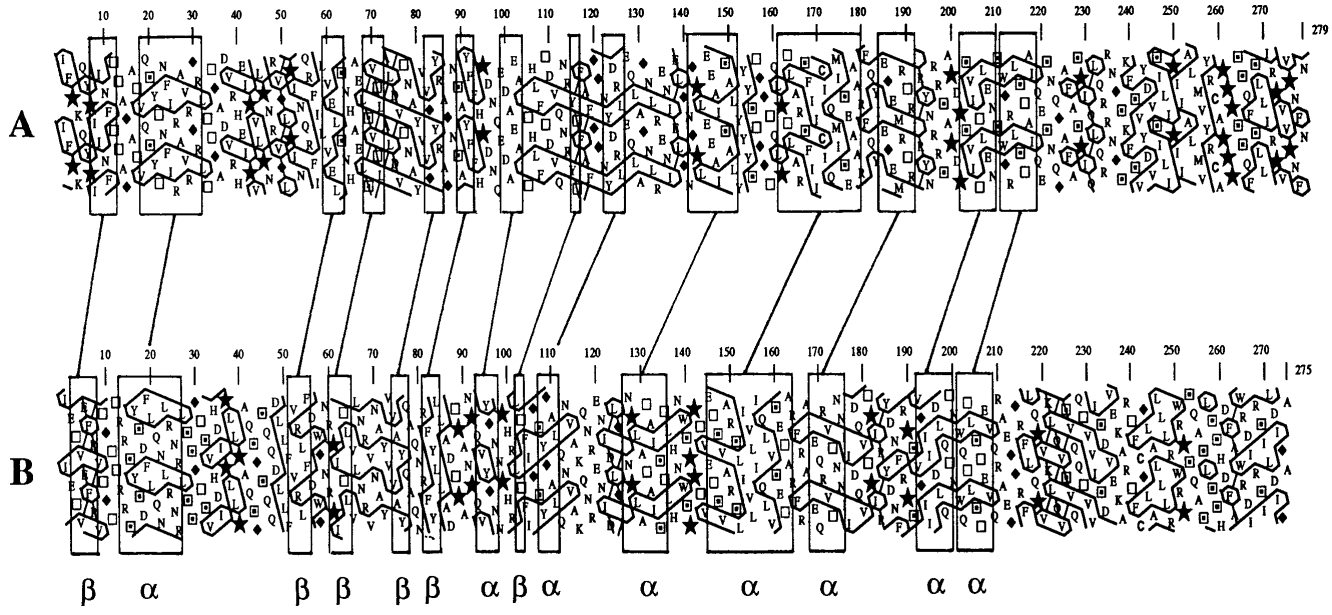

Figure 4 Comparison of the HCA plots of the A-chain of ricin (A) and IrisRIP.A3 (B)

Helices (α) and strands of β-sheet (β) delineated on the HCA plot of ricin A-chain were reported on the HCA plot of IrisRIP.A3. These delineations were used to recognize the structurally conserved regions between the ricin A-chain and IrisRIP.A3.

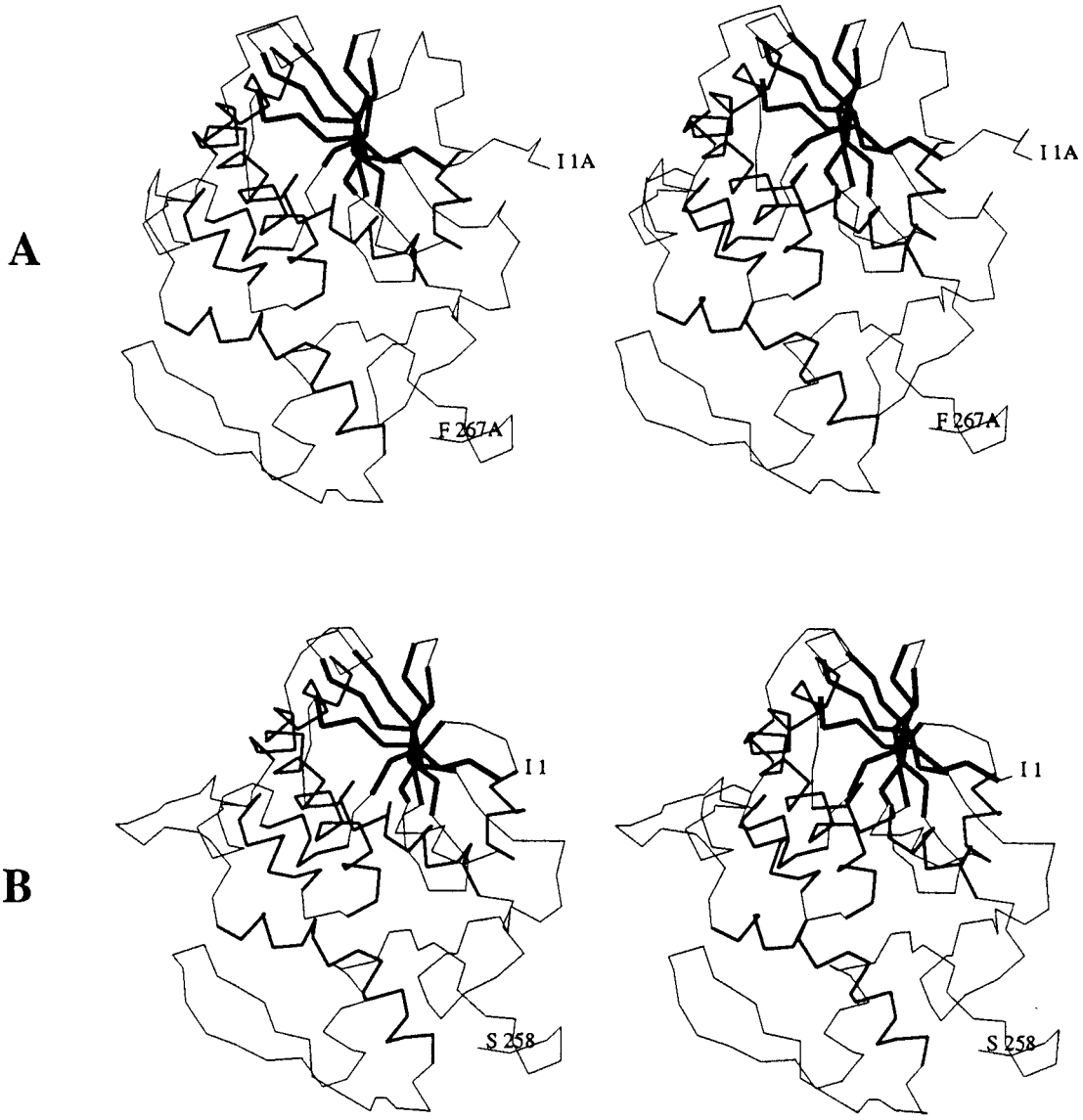

Figure 5 Stereoviews of the three-dimensional models of ricin A-chain (A) and IrisRIP.A3 (B)

Helices (thick lines) and left-handed twisted 6-strand β-sheet (heavy lines) are indicated. The deep cleft shown on the right side of the chains corresponds to the active site which binds adenine of 28S RNA.

1300 nucleotides (results not shown). Identical results were obtained when hybridization was performed with the random-primer-labelled cDNA clones encoding the *Iris* RIP. The size of the RNA is in good agreement with the length of the cDNA clones that were analysed.

Molecular modelling

The amino acid sequences of the type 1 RIP from *Iris* exhibit a high degree of identity and similarity with other type 1 RIPs and with the A-chains of type 2 RIPs. RIPIriHol.A3, for instance, has 35% identity and 62% similarity with the A-chain of the classical type 2 RIP ricin. Since the high degree of similarity between this type 1 RIP and the A-chain of ricin indicates that both polypeptides are closely related structurally, the sequence RIPIriHol.A3 encoding IrisRIP.A3 was modelled using the co-ordinates of ricin, the three-dimensional structure of which has been resolved by X-ray crystallography [20]. Although it must be emphasized that the results of these modelling studies have to be interpreted with care, they can give interesting information about structural similarities between related proteins.

The catalytically active A-chain of ricin is built up of three distinct domains and contains regular secondary structures such as eight α-helices, and six strands of β-sheet, which exhibit a left-handed twist of approx. 110 ° when observed along the hydrogen bonds [23]. A comparison of the HCA plots of the A-chain of ricin and IrisRIP.A3 shows that α-helices and strands of β-sheet are readily conserved in both proteins, although some discrepancies exist between both sequences due to gaps or insertions of a few amino acid residues occurring between the secondary-structure features of IrisRIP.A3 (Figure 4). Once the structurally conserved regions common to both proteins were identified, the coordinates of ricin could be used to build a three-dimensional model of IrisRIP.A3.

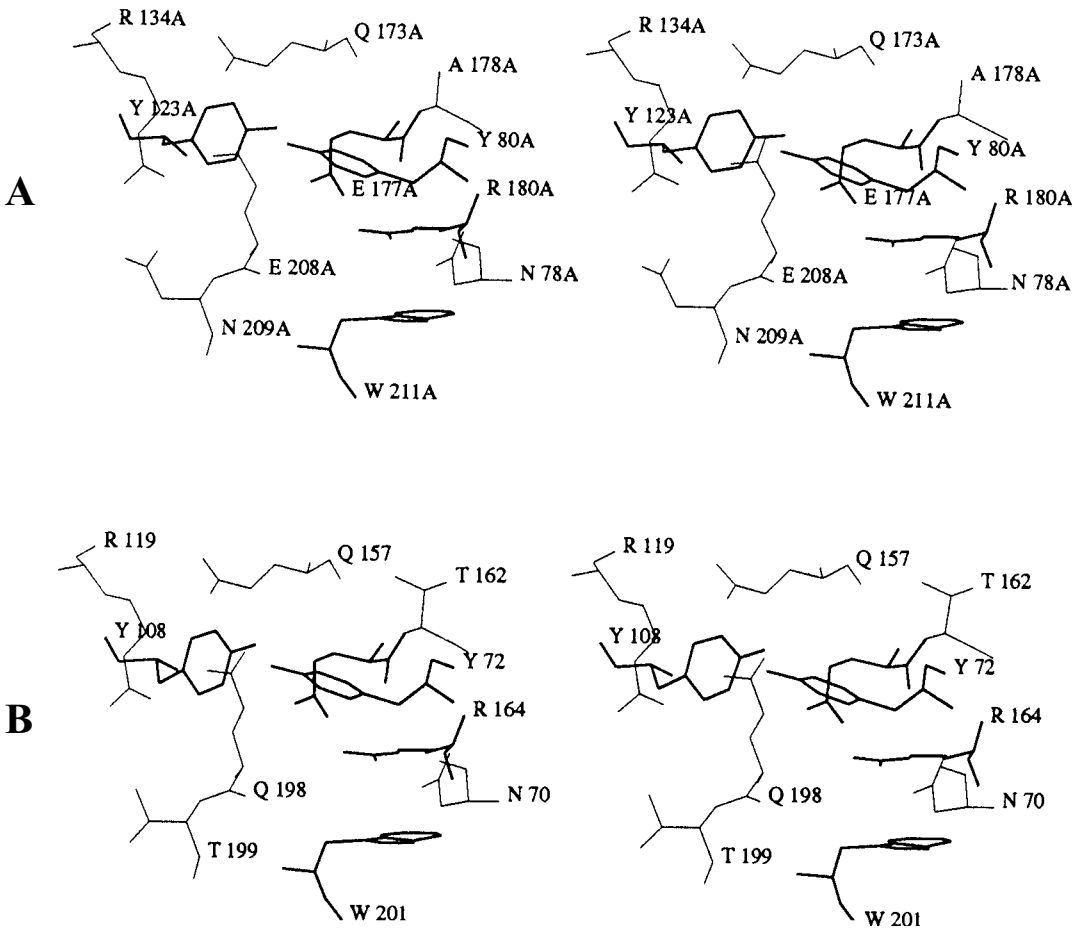

Figure 6 Stereoviews of the active site of ricin A-chain (A) and IrisRIP.A3 (B)

The stereoviews show the amino acid residues involved in the binding of adenine (thick lines) together with the residues associated with the site (thin lines).

Modelling of IrisRIP.A3 yielded a three-dimensional model very similar to that of the ricin A-chain (Figure 5). Despite a few discrepancies due to the deletions and insertions between the secondary structures, the overall folding of the ricin A-chain is fully conserved in IrisRIP.A3. IrisRIP.A3 contains eight α-helices and a six-stranded β-sheet with a left-handed twist similar to those found in the ricin A-chain.

All amino acid residues that build up the active site of the A-chain of ricin (Tyr^{80}, Tyr^{123}, Glu^{177}, Arg^{180} and Trp^{211}) [23–25] are fully conserved in IrisRIP.A3 (Tyr^{72}, Tyr^{108}, Glu^{161}, Arg^{164} and Trp^{201}). However, Ala^{178}, another invariant residue, which is conserved in all A-chains and is probably responsible for the stable state of the active site of the ricin A-chain [23], is replaced by Thr^{162} in IrisRIP.A3, as well as in all other type 1 RIPs from *Iris*. With the exception of two changes, all residues that are located in the vicinity of the active site of the ricin A-chain, and are probably necessary to maintain its catalytic conformation (Asn^{78}, Arg^{134}, Gln^{173}, Glu^{208} and Asn^{209}), are conserved in IrisRIP.A3 (Asn^{70}, Arg^{119}, Gln^{157}, Gln^{198} and Thr^{199}) (Figure 6). This high degree of conservation is in good agreement with the RIP activity of IrisRIP.A3.

Because of the high degree of both sequence identity ($> 85\%$) and similarity ($> 95\%$) between the three type 1 RIP isoforms from *Iris*, all these proteins exhibit a three-dimensional structure that is very similar to that of the ricin A-chain, and their HCA plots are almost identical (results not shown). Like in IrisRIP.A3, the residues responsible for the N-glycosidase activity of the ricin A-chain are also conserved in the other two isoforms, except for Ala^{178}, which is replaced by Thr^{162}.

The three-dimensional models of the *Iris* sequences, built from the co-ordinates of ricin, can nicely be superimposed on the structures of the type 1 RIP trichosanthin (PDB code 1mrj) and momordin I (α-momorcharin, PDB code 1mri) [26], and on that of the A-chain of abrin (PDB code 1abr) [27] (Figure 7). This holds especially true (r.m.s. deviation < 0.5 Å) for the α-helices and strands of β-sheet, which constitute the overall folding pattern of the proteins. The only discrepancies occur in the loop conformations. As a result, the network of amino acid residues forming the adenine-binding site of all these protein models is well superimposable.

Phylogenetic tree

A search in the database indicated that the deduced amino acid sequences of the type 1 RIP from *Iris* exhibit a high degree of sequence similarity to the previously cloned type 1 RIPs, as well as to the A-chains of type 2 RIPs. As shown in Figure 8, the *Iris* RIPs form a separate cluster of the phylogenetic tree built from the amino acid sequences of various type 1 RIPs and the A-chains of type 2 RIPs. It is also noteworthy that the type 1 RIPs

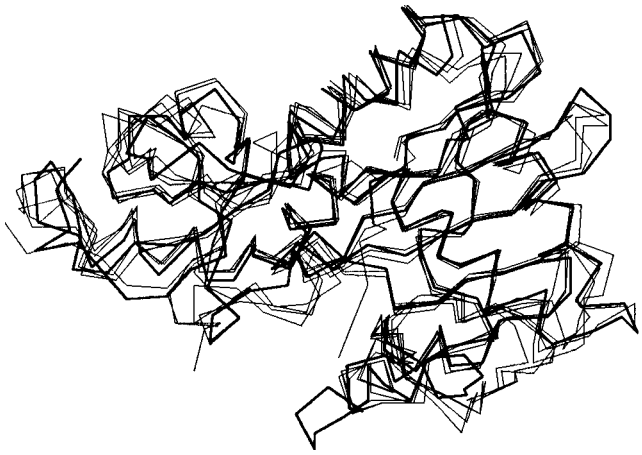

Figure 7 Superimposition of the three-dimensional models of IrisRIP.A3 (thick line) with those of the A-chains of ricin and abrin, as well as the type 1 RIPs α-momorcharin and trichosanthin (thin lines)

The secondary-structure features (α-helices and β-sheets) are well superimposed. Most of the discrepancies occur in the loop regions.

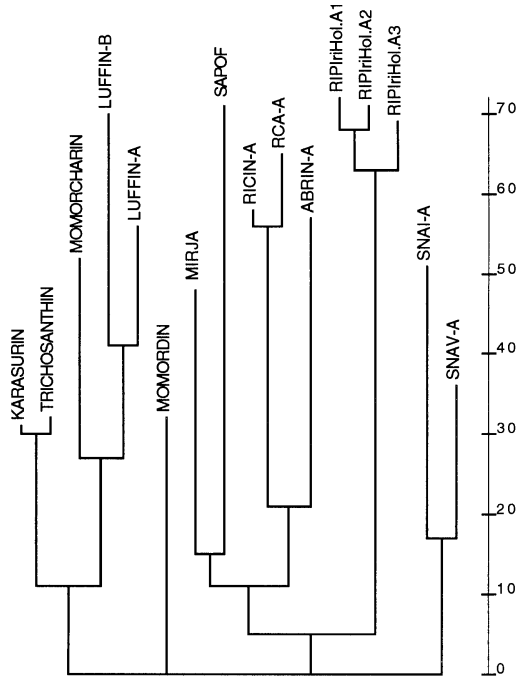

Figure 8 Phylogenetic tree built up from the amino acid sequences of different RIPs

The phylogenetic tree is built from the sequences of *Iris hollandica* (RIPIriHol.A1, RIPIriHol.A2 and RIPIriHol.A3), *Luffa cylindrica* (luffin-a and luffin-b), *Trichosanthes kirilowii* (trichosanthin, karasurin), *Momordica charantia* (momorcharin), *Momordica balsamina* (momordin), *Mirabilis jalapa* (mirja), *Saponaria officinalis* S6 (sapof) and the A-chains from the type 2 RIPs of *Ricinus communis* (Ricin-A and RCA-A), *Abrus precatorius* (Abrin-A) and *Sambucus nigra* (SNAI-A and SNAV-A). The scale indicates the number of amino acid changes.

from *Iris* are apparently more closely related to the type 2 RIPs from *Abrus precatorius* and *Ricinus communis* than to most other type 1 RIPs.

DISCUSSION

The present paper describes the isolation and molecular cloning of three isoforms of a protein from the bulbs of *Iris* that could be identified as type 1 RIPs on the basis of their inhibitory effect on cell-free protein synthesis and the release of adenine from ribosomes. Like other RIPs, they act not only on whole ribosomes, but also on purified rRNA, poly(A) and DNA, confirming that at least the effect on DNA is a common property of all RIPs tested so far [6]. Sequence comparisons and molecular modelling indicated that the *Iris* RIPs are structurally and evolutionary related to type 1 RIPs from other species and to the A-chain of type 2 RIPs. The discovery of the *Iris* RIPs is important since it demonstrates for the first time that the occurrence of these proteins within the monocotyledoneae is not restricted to the Gramineae (like wheat, barley, rye, rice and maize) and Asparagaceae (asparagus). In addition, the identification of the most abundant bulb protein as a type 1 RIP shows that not only seeds but also typical vegetative storage organs can accumulate large quantities of a presumably defence-related protein. The latter observation has two important consequences. First, *Iris* bulbs are a readily available and rich source of a type 1 RIP that can easily be isolated by simple techniques. Secondly, the high concentration of type 1 RIPs in the bulbs addresses the question of their physiological role. By analogy with the double role of some abundant plant lectins [28], the hypothesis can be put forward that the *Iris* type 1 RIPs are storage proteins, which due to their particular enzymic activity can be used as defence proteins whenever the plant is challenged by a pathogen or a predator. It is evident, however, that such a defence-related role does not preclude another more specific role in the metabolism of the plant.

REFERENCES

1 Barbieri, L., Battelli, M. G. and Stirpe, F. (1993) Biochim. Biophys. Acta **1154**, 237–282
2 Endo, Y., Tsurgi, K. and Lambert, J. M. (1988) Biochem. Biophys. Res. Commun. **150**, 1032–1036
3 Barbieri, L., Gorini, P., Valbonesi, P., Castiglioni, P. and Stirpe, F. (1994) Nature (London) **372**, 624
4 Barbieri, L., Valbonesi, P., Gorini, P., Pession, A. and Stirpe, F. (1996) Biochem. J. **319**, 507–513
5 Stirpe, F., Barbieri, L., Gorini, P., Valbonesi, P., Bolognesi, A. and Polito, L. (1996) FEBS Lett. **382**, 309–312
6 Barbieri, L., Valbonesi, P., Bonora, E., Gorini, P., Bolognesi, A. and Stirpe, F. (1997) Nucleic Acids Res. **25**, 518–522
7 Dubois, M., Gilles, K. A., Hamilton, J. K., Rebers, P. A. and Smith, F. (1956) Anal. Chem. **28**, 350–356
8 Laemmli, U.K. (1970) Nature (London) **227**, 680–685
9 Parente, A., De Luca, P., Bolognesi, A., Barbieri, L., Battelli, M. G., Abbondanza, A., Sande, M. J. W., Gigliano, G. S., Tazzari, P. L. and Stirpe, F. (1993) Biochim. Biophys. Acta **1216**, 43–49
10 Ferreras, J. M., Barbieri, L., Girbés, T., Battelli, M. G., Rojo, M. A., Arias, R. J., Rocher, M. A., Soriano, F., Mendéz, E. and Stirpe, F. (1993) Biochim. Biophys. Acta **1216**, 31–42
11 Zamboni, M. C., Brigotti, M., Rambelli, F., Montanaro, L. and Sperti, S. (1989) Biochem. J. **259**, 639–643
12 McCann, W. P., Hall, L. M., Siler, W., Barton, N. and Whitley, R. J. (1985) Antimicrob. Agents Chemother. **28**, 265–273
13 Van Damme, E. J. M. and Peumans, W. J. (1993) in Lectins and Glycobiology (Gabius, H.-J. and Gabius, S., eds.), pp. 458–468, Springer Verlag, Berlin
14 Van Damme, E. J. M., Kaku, H., Perini, F., Goldstein, I. J., Peeters, B., Yagi, F., Decock, B. and Peumans, W. J. (1991) Eur. J. Biochem. **202**, 23–30
15 Mierendorf, R. C. and Pfeffer, D. (1987) Methods Enzymol. **152**, 556–562
16 Sanger, F., Nicklen, S. and Coulson, A. R. (1977) Proc. Natl. Acad. Sci. U.S.A. **74**, 5463–5467
17 Maniatis, T., Fritsch, E. F. and Sambrook, J. (1982) Molecular Cloning: A Laboratory Manual, Cold Spring Harbor Laboratory, Cold Spring Harbor, NY
18 Gaboriaud, C., Bissery, V., Benchetrit, T. and Mornon, J. P. (1987) FEBS Lett. **224**, 149–155

19 Lemesle-Varloot, L., Henrissat, B., Gaboriaud, C., Bissery, V., Morgat, A. and Mornon, J. P. (1990) Biochimie **72**, 555–574
20 Rutenber, E., Katzin, B. J., Collins, E. J., MIsna, D., Ready, M. P. and Robertus, J. D. (1991) Proteins **10**, 240–250
21 Maddison, W. P. and Maddison, D. R. (1992) MacClade: Analysis of Phylogeny and Character Evolution, Version 3.0, Sinauer Associates, Sunderland, MA, U.S.A.
22 von Heijne, G. (1986) Nucleic Acids Res. **11**, 4683–4690
23 Katzin, B. J., Collins, E. J. and Robertus, J. D. (1991) Proteins **10**, 251–259
24 Kim, Y. and Robertus, J. D. (1992) Protein Eng. **5**, 775–779
25 Chaddock, J. A. and Roberts, L. M. (1993) Protein Eng. **6**, 425–431
26 Huang, Q., Liu, S., Tang, Y., Jin, S. and Wang, Y. (1995) Biochem. J. **309**, 285–298
27 Tahirov, T. H., Lu, T. H., Liaw, Y. C., Chen, Y. L. and Lin, J. Y. (1995) J. Mol. Biol. **250**, 354–367
28 Peumans, W. J. and Van Damme, E. J. M. (1995) Plant Physiol. **109**, 347–352

Received 13 January 1997/20 February 1997; accepted 21 February 1997